Hydrodynamic loads induced by a gravity current on a submerged circular cylinder.

E.V.Ermanyuk , N.V.Gavrilov.

Lavrentyev Institute of Hydrodynamics, 630090 Novosibirsk, Russia, ermanyuk@hydro.nsc.ru

Summary

This paper presents the experimental study of forces induced by a gravity current on a submerged circular cylinder. It is shown that under experimental conditions loads are similar in the sense of the Froude modeling. Maximum loading occurs when the gravity current interacts with a cylinder laying on the bottom. The maximum hydrodynamic load decreases as the gap between the cylinder and the bottom increases.

1 Introduction

Gravity currents take place in many natural situations. The extreme forms of gravity currents, such as snow avalanches or pyroclastic flows produced by volcanic eruptions, present a severe natural hazard. Relatively 'mild' forms of gravity currents represented by the motion of athmospheric fronts have a strong impact on the safety of aircraft operations. In ocean, gravity currents occur as buoyancy-driven flows due to salinity or temperature inhomogeneities, or as turbidity currents where the density difference is due to suspended particles. Such currents present a significant hazard to submerged vehicles, pipelines and cables.

The structure of the gravity-current heads and their speeds of propagation have been studied in some detail (see reviews in [1, 2]). However, although some authors [1, 3–5] have studied the interaction of gravity currents with submerged obstacles, little is known on hydrodynamic loads induced by the gravity currents. This report presents the experimental study of loads produced by an inertial gravity current on a submerged circular cylinder.

2 Experimental setup and procedure

The scheme of experimental setup is shown in fig. 1 Experiments were carried out in a test tank of length $320cm$, width $20cm$ and depth $14cm$. The vertical slide gate *1* divides the tank in two equal parts. The left part of the tank was filled to the depth H with pure water of density ρ_1. The right part of the tank was filled with a two-fluid system: the lower layer of sugar-water solution of depth h_2 and density ρ_2 and the upper layer of pure water with density ρ_1 and depth h_1 so that $h_1 + h_2 = H$. Body *2* was installed in the right side of the test tank. The lower and upper edges of body *2* were located at the distances h_0 and h_2 from the bottom, respectively. In experiments the values of geometrical parameters were fixed as $H = 12cm$, $h_2 = 8cm$, $h_0 = 2.3cm$. Once the slide gate *1* was removed, the gravity current *3* propagated to the left in the left part of the tank, while the depression wave *4* propagated to the right in the right part of the tank. The hydrodynamic loads induced by the gravity current on the submerged circular cylinder *5* of diameter $D = 1.5cm$ were measured by two-component balance *6*. The natural frequencies of the balance were about $30Hz$. The center of cylinder *5* was located at distance d from the bottom and $l = 4H$ from the slide gate. The output from the force sensors was recorded and stored by a computer with 12-bit analog-to-digital converter. The flow pattern was registered by a digital camera.

3 Experimental results

In the zone of the force measurements (at the distance $4H$ from the slide gate) the gravity current is in the stage of well-developed inertial regime characterized by practically constant speed V of the gravity current

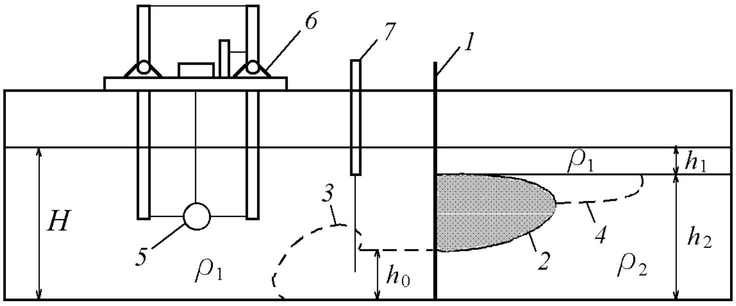

Figure 1: Experimental setup

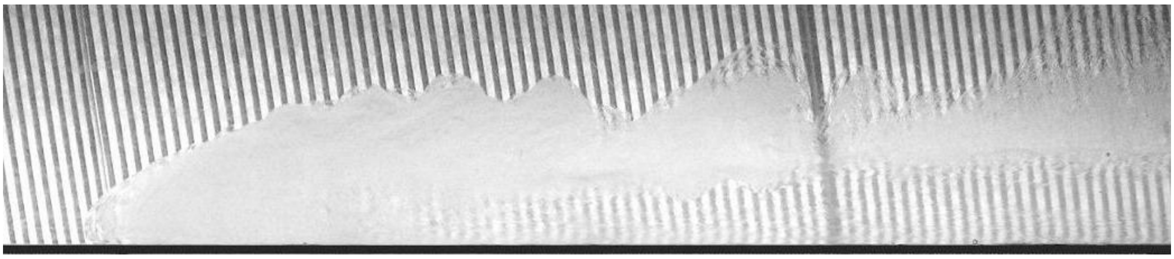

Figure 2: Flow structure of inertial gravity current

head (the main flow regimes of gravity currents are discussed in [1]). Usually, the speed of the current front is represented as dependence of the Froude number $\mathrm{Fr} = V/(\epsilon g h_*)^{1/2}$ on $\alpha = h_*/H$, where $\epsilon = (\rho_2 - \rho_1)/\rho_1$, g is the gravity acceleration, h_* is the vertical size of the core region of the gravity current. The function $\mathrm{Fr}(\alpha)$ was first obtained in [6] for a two-layer system of ideal immiscible fluids.

For a two-layer system of miscible viscous fluids the data on $\mathrm{Fr}(\alpha)$ can be found in [1] (see figure 11.11). The typical flow pattern in the gravity current is shown in fig. 2. The head of the gravity current is well-mixed, with the height about $2h_*$. Visualization shows that the vertical size of the core region can be taken as $h_* = h_0$. The speed of the lower fluid in the core region is $V_0 \approx 1.2V_*$. Above the core region, there is a mixed zone with the vertical size about $0.7h_*$. For the present experimental conditions $\mathrm{Fr} = 0.82$, what is in good agreement with the data [1] for $\alpha = h_*/H = 0.19$.

A typical pattern of the gravity flow interacting with the submerged cylinder is shown in fig. 3 for $d/D = 0.8$ and $\epsilon = 0.02$. One can see a considerable elevation of the mixed fluid level above the cylinder and a strong jet below the cylinder. The initial stage of the interaction between the gravity current and the

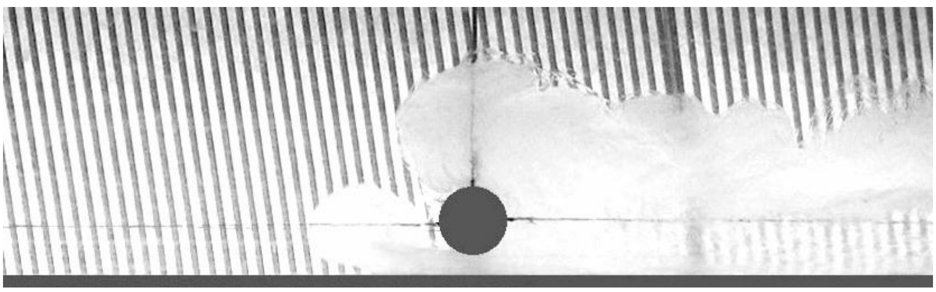

Figure 3: Interaction of inertial gravity current with submerged cylinder

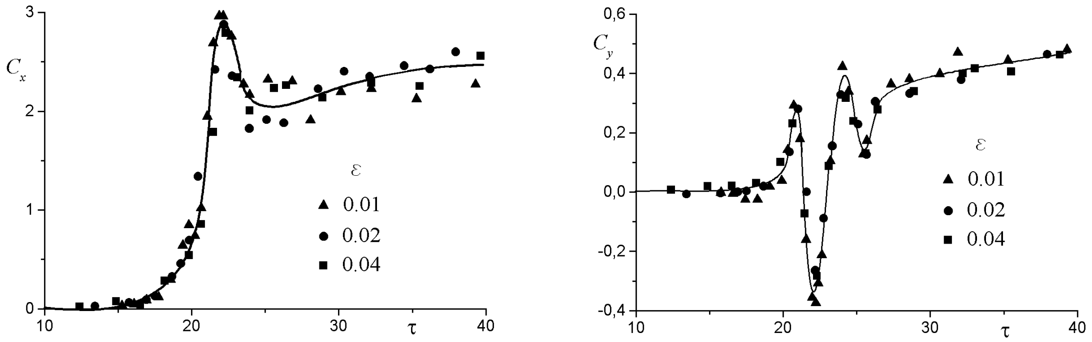

Figure 4: Force coefficients C_x and C_y versus non-dimensional time τ at different ϵ. Smoothed universal dependencies are shown by solid lines.

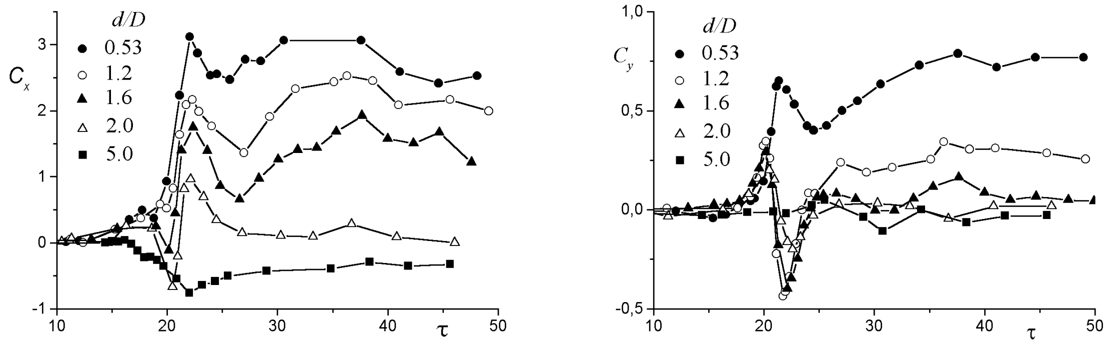

Figure 5: Time-histories of force coefficients $C_x(\tau)$ and $C_y(\tau)$ for different distances d/D of the cylinder center from the bottom

cylinder reminds the impact of a body onto a free surface. The time-scale of the interface elevation near the cylinder can be taken as $T = (h_0/\epsilon g)^{1/2}$. We can assume that horizontal and vertical hydrodynamic loads per unit length of the cylinder F_x and F_y are proportional to $\rho V^2 D$. The force component due to the difference of hydrostatic pressures at different sides of the obstacle is proportional to $\rho\epsilon g D^2$. For fixed geometrical parameters of the problem and different ϵ, one can expect $F_{x,y} \sim \epsilon$ and $T \sim \epsilon^{-1/2}$. Thus, we assume that global similarity in Froude number guarantees similarity of mixing processes and the effects of Reynolds number variation and stochastic disturbances due to shear instability at the upper boundary of the gravity current are minor. This assertion was proved in a set of experiments conducted for $\epsilon = 0.01; 0.02; 0.04$ at fixed $d/D = 0.8$.

The results of this series are presented in fig. 4 as force coefficients per unit length $C_{x,y} = 4F_{x,y}/(\rho\epsilon g\pi D^2)$ versus non-dimensional time $\tau = t(\epsilon g/h_0)^{1/2}$. The moment when the gravity current passes the wave meter *7* is taken as $\tau = 0$. One can see that, although the flow patterns shown in figs. 2 and 3 are complicated by mixing and shear instability, the time-history of the hydrodynamic force is essentially a well-determined process governed by the balance of inertia and buoyancy. Note that when ϵ varies between 0.01 and 0.04 the Reynolds number defined as $Re = Vh_*/\nu$ (where ν is the kinematic viscosity) varies in a narrow range between 770 and 900 since ν increases with ϵ.

The time-histories $C_{x,y}(\tau)$ of the force coefficients are presented in fig. 5 for different distances between the cylinder and the bottom d/D. These results were obtained at $\epsilon = 0.02$. For any d/D the horizontal load is several times higher than the vertical one. Maximum forces take place when cylinder practically touches the bottom ($d/D \approx 0.5$). It is interesting to note that the maximum horizontal force at $d/D \approx 0.5$

is approximately equal to the load produced on an infinite vertical wall by a horizontal jet of thickness h_0 moving with velocity V_0. It should be also noted that the vertical force at $d/D \approx 0.5$ is positive at any τ. This is the effect of the suction force from the current flowing above the cylinder. For higher d/D the flow goes both above and below the cylinder (as in fig. 3), and the vertical force coefficient C_y has oscillatory behavior, and takes positive and negative valuies. The maximum forces markedly decrease as d/D increases.

Experiments were also conducted with the gravity current advancing over a thin layer of fluid of density ρ_2. The head of such a current propagates in the form of a smooth undulatory bore. Typical hydrodynamic loads in this case are smaller than in the above-described case, and the typical time-scales of force oscillations are longer.

4 Acknowledgements

The study was partially supported by the Integration Project of SB RAS under grant No. 3.13.1.

References

[1] Simpson J.E.(1997) *Gravity currents: in the environment and the laboratory.* Cambridge: Cambridge University Press.

[2] Thomas L.P., Dalziel S.B., Marino B.M. (2003) The structure of the head of an inertial gravity current determined by particle-tracking velocimetry *Exp. Fluids* **34**, 708–716.

[3] Rottman J.W., Simpson J.E., Hunt J.S.R., Britter R.E. (1985) Unsteady gravity currents over obstacles *J. Hazardous Mat.* **11**, 325–340.

[4] Greenspan H.P., Young R.E. (1978) Flow over a containment dyke. *J. Fluid Mech.* **87**, 179–192.

[5] Lane-Serff G.F., Beal L.M., Hadfield T.D. (1995) Gravity current flow over obstacles. *J. Fluid Mech.* **292**, 39–53.

[6] Benjamin T.B. (1968) Gravity currents and related phenomena. *J. Fluid Mech.* **31**, 209–248.